HEFAT2014
10th International Conference on Heat Transfer, Fluid Mechanics and Thermodynamics
14 – 16 July 2014
Orlando, Florida

MODELLING OF HEAT TRANSFER IN HUMAN EYE USING COMPUTATIONAL FLUID DYNAMICS TECHNIQUE

Samanta S*, Sinha M.K*, Bhushan V and Kumar P
*Authors for correspondence
Department of Mechanical Engineering,
National Institute of Technology, Jamshedpur,
Jamshedpur, 831014,
India,
E-mail: sauradeepsamanta@yahoo.com

ABSTRACT

Thermal modelling of the eye is important as it can provide us with a tool to determine the effect of external heat sources on the eye as well as to direct any abnormalities developed in the eye, as can be inferred from any deviation in the steady state temperature distribution inside the eye. It is seen that increase in blood flow in the anterior segment of the eye can increase the corneal temperature by 2.4˚C and a decrease in the blood flow in the anterior segment as well as in case of Carotid artery disease can reduce the corneal temperature by 1.3˚C. Moreover, in order to optimize laser therapy in ophthalmology, it is essential to have a better understanding of the thermal response of different sections of the eye for an imposed heat flux. In the present paper, the Computational Fluid Dynamics method is applied to analyse the steady state temperature distribution in a two-dimensional model of the human eye. For accomplishing this objective, computational fluid dynamics technique is to be used using Fluent and ICEM CFD meshing. In this study, the temperature distribution is determined in the normal unexposed human eye with a two dimensional model which is assumed to be symmetric at the pupillary axis. It consists of seven regions with boundary conditions employed on the surface of the cornea and the sclera. The results were verified with experimental and computational results obtained by previous studies on human as well as animal eyes. However because of experimental constraints the computational approach has been taken care of while considering the experimental results obtained. It is seen that the temperature distribution is different for the front and rear surface of the cornea. Also there is a variation in the temperature in the range of 34.23˚C to 34.5˚C for the cornea. The steady state temperature distribution obtained could be used unanimously with medical science to treat different diseases like cataracts, glaucoma and to list down precautions to be taken during tender state of eye especially after surgeries.

INTRODUCTION

The number of cases relating to Eye infections and diseases has escalated in the recent years. The reasons behind this are associated with the unhealthy habits and routines being followed by the society along with complex and continuously changing environmental conditions prevailing in the new world. Mathematical and Computational models are the tools for studying of the biological systems and may be used for early diagnosis of eye diseases. This is very important for treatment of the diseases in a more effective manner by the ophthalmologist.

In the last few decades, the exposure of mankind to radiation has increased drastically, and eye is one of the most sensitive organs to this radiation. Since there is no skin layer to absorb radiation from wireless networks or electromagnetic waves, the eye is particularly sensitive to heating from these sources. In addition, the deficiency of blood flow into the eye subject it to thermal damage even in the presence of mild heating, which could potentially lead to clouding or reduced transparency of the lens, or cataract. In many pathological conditions, loss of pigment from the iris occurs (e.g., pigmentary glaucoma) which normally occurs with advancing age. The aqueous humour circulating through the posterior and anterior chambers carries liberated pigment which is deposited on the iris, lens and posterior surface of the cornea. The pigment deposited on the posterior cornea surface is in the form of a vertical line called Krukenberg's spindle [1]. As a result of heavy pigmentation of its endothelial surface, damage to the cornea may occur, including blockage of the corneal dehydration mechanism leading to edema [2]. The cornea is cooled by the surrounding air and by evaporation of the tear film to a temperature less than 37˚C [3]. A temperature gradient is created in the eye by cooling of the cornea, which causes thermal convection currents in the anterior chamber that are hypothesized to be responsible for the formation of a spindle of

pigment. Research on the temperature gradients of the eye date back to last century, but heat transfer models of the eye have only been developed during the past three decades. One of the initial models of the eye was developed by Al-Badwaihy and Youssef [4] in 1976 to analyse the thermal effects of microwave radiation on the eye. The eye was modelled as a spherical structure composed of uniform tissue, and thermal properties were obtained from averaging the thermal properties of individual ocular tissues. The analytical solution was developed for steady state conditions.

In previous thermal models of the eye, heat transfer in different parts was primarily modelled using conduction and in a few cases by natural convection. Ooi and Ng studied the effect of aqueous humour hydrodynamics on the heat transfer within the eye [5]. They also investigated the effect of different variables on the thermal modelling of the eye using boundary element approach where they established the corneal centre temperature numerically along with normal heat flux [6]. They also made a study on 2D eye with the bio heat equation using FEM [7]. Lagendijk [8] performed experiments on the normal and heated rabbit eye and developed a conduction model to achieve the temperature distribution in human and rabbit eyes.

Scott [9] utilized a two-dimensional finite element method to obtain the temperature profile based on heat conduction in different sections of the eye. Effect of lens thermal conductivity, evaporation from cornea surface, blood flow in choroid, ambient temperature, ambient convection coefficient and blood temperature on the eye temperature distribution was studied based on a conduction model. Using a two dimensional model, Scott also calculated the temperature change in intra-ocular media subjected to an infrared radiation. Along with this a heat transfer model has been developed using Web-Spline technique by Kunter and Seker [10].However in this model internal heat generation in the cornea due to tear evaporation has not been taken into consideration. Moreover, Cicekli also developed a 2D heat transfer model using FEM making use of ABAQUS[11]. Mapstone[12] recorded the cornea temperature subject to different ambient temperatures. . In the experiment that was conducted by Mapstone (1968) taking temperatures with the bolometer, the corneal temperature increased up to 1.0˚C. The reason for this kind of increase in temperature was because due to either voluntary lid retraction to expose the necessary amount of the cornea or by manipulation of the lids by the experimenter. Tears may have also a cooling effect on the cornea if they evaporate from the pre-corneal film. The superficial oily layer of the pre-corneal film protects against evaporation from the inner fluid layer, It was shown experimentally that any imperfection in the oily layer causes the increase in evaporation rate between 2.2-3.7μ to 40-45 μ. Humidity is also one of the effects that cause evaporation, which was found to be a small quantity, 1 per cent. It also causes cooling effect on the cornea. The two overall effects of tears on the corneal temperature are: first, the cooling effect because of evaporation of tears from the pre-corneal film, second, a heating effect because of the secretion of warm tears and their path across the front of the colder cornea. If there is normal secretion of the tears in the eye, it is not expected to be an effect from the tears in the corneal temperature.

Hence in many models of the eye an assumption is made that it is homogeneous and that the material parameters of the eye can be approximated to those of water. However, heat flow across the thin (~ 0.8 mm thick) cornea has been shown to be significantly lower than if the same layer consisted of water. One of the primary reasons for the lack of accurate material parameters of the eye is the difficulty in conducting direct experiments on the human eye. Instead, properties of animal eyes have been measured. A porcine eye was tested by (Kampmeier 2000)[13] and (Sporl 1997) or on rabbit eye by Tanelian and Beuerman (1984)[14]. The reason for using an eye for these animals is because of their similarity and having close material parameters to those of the human eye.

In this study, normal behavior of the eye under prevailing environmental conditions and blood perfusion is being studied by making use of a 2D model of the eye along with any variation in the environmental temperature or the blood perfusion rate on the steady state temperature distribution. Finite element approaches have been performed in the past as discussed earlier however, there are no well-established Simulation approaches that can quantify and summarize every aspect of heat transfer phenomenon, i.e. both thermal and fluid aspect, occurring within the eye. At the elementary level, the two-dimensional model of the eye has been considered with an assumption that the eye is symmetrical about the pupillary axis. Thus the model consists of 7 sections with individual properties of Cornea, Lens, Iris, Blood, Aqueous Humour, Sclera and Vitreous Humour. Efforts have been made to develop an accurate model and solve the computational model with proper conditions, however, we do not claim the model to be perfect but the computational model can help the researchers get a better picture of the thermal and fluidic mechanisms occurring within the eye.

NOMENCLATURE

C	[J/kgK]	Specific heat of the medium
k	[W/mK]	Thermal conductivity
Q	[W/m^3]	Volumetric heat generation density
h	[W/m^{2}K]	Convective heat transfer coefficient
E	[W/m^2]	Loss in heat flux due to evaporation of tears
t	[s]	Time
T	[K]	Temperature
n	[-]	Unit vector normal to a surface
V	[m/s]	Velocity of the fluid
u	[m/s]	x-component of velocity
v	[m/s]	y-component of velocity
Special Characters		
ρ	[kg/m^3]	Density of the medium
ω	[m^3/s]	Blood flow rate
ε	[-]	Corneal Emissivity
σ	[W/m^{2}K^4]	Stefan-Boltzmann constant
Subscripts		
t		Tissue
b		Blood
a,in		Arterial inlet
v,out		Venous outlet
$blood$		Blood properties
ambient		Ambient or reference
1		Properties of region 1
2		Properties of region 2

EYE ANATOMY AND THERMAL PROPERTIES

In order to understand the development of the models, a basic understanding of eye anatomy is necessary. The eye is a complex optical system. A relatively small organ in the human body, the eye is a passageway to understanding and emotion. Not only does the eye allows us to see and interpret the shapes, colours, and dimensions of objects in the world by processing the light they reflect or emit, but it also enables us to see and interpret unspoken words and unexplainable environments. It acts as a transducer as it changes light rays into electrical signals and transmits them to the brain, which interprets these electrical signals as visual images. The anterior portion of the eye includes the cornea (the clear outer covering of the eye), anterior chamber (filled with aqueous humour), and the iris. The posterior portion of the eye includes the lens, ciliary bodies (tissue that holds the lens to the sclera), vitreous chamber (filled with vitreous humour), retina (light-sensitive back of the eye), and sclera (white part of the eye). Blood flow occurs only in the back of the eye, in the sclera and retina region with a minor supplement to the iris. In Figure 1 it can be seen that the eye is approximately a spherical organ. The back surface is covered with a thin membrane (retina) that is permeated with blood vessels and is connected with the brain by the optic nerve. Under the retina is a layer called the choroid which serves to nourish it. The lens lies between the aqueous humour and vitreous humour. The aqueous and vitreous humours are transparent liquids with different concentrations of Sodium Chloride (NaCl). Figure 1[15] highlights most of the key features in the eye included in the model to be discussed.

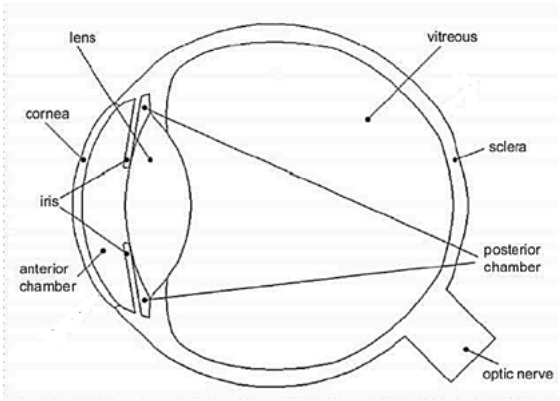

Figure 1 Physical representation of 2D model of eye.

Different authors have represented the 2D section of the eye in a somewhat different manner however following figures, i.e., figure 1, figure 2[16] and figure 3[17] give a very vivid description of the various components of the eye along with the relevant dimensions of each of the components with reference to a 2D section. Figure 3 represents blood circulation within the eye which plays an important role in the heat transfer phenomenon.

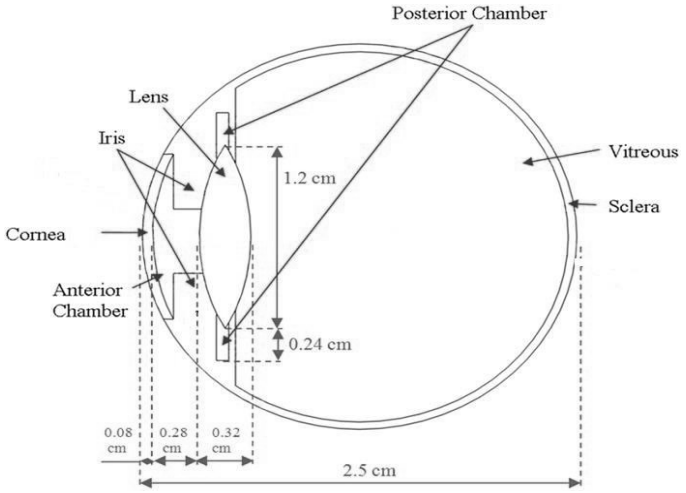

Figure 2 Physical representation of eye with dimensions.

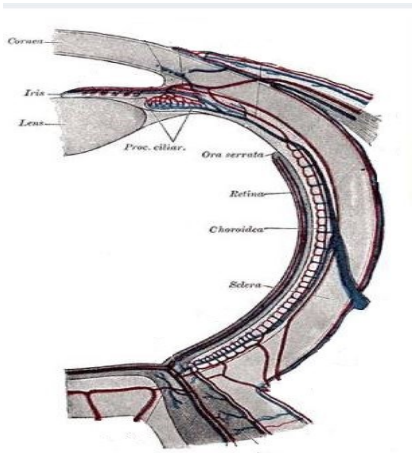

Figure 3 Physical representation of blood circulation within the eye.

In this study, thermal properties of the various components of the eye have been taken into consideration that is shown in table 1[11].

Table 1 Material Properties of the eye

Sub Domain	Thermal Conductivity [W/mK]	Specific Heat [J/kgK]	Density [kg/m^3]
Cornea	0.35	3642.5	1062
Aqueous	0.5779	4180	996
Sclera	1.004	3182	1100
Lens	0.3998	3001.93	1000
Iris	1.004	3182	1100
Vitreous	0.5779	4180	996
Water	0.6	4182	998.2
Blood	0.505	4186	1060

MATHEMATICAL MODELLING AND METHOD

Mathematical Modelling of Human Eye

In reality, in between the subdomains of sclera and the vitreous, one may find two tissue layers known as the retina and the choroid. For simplicity, since these layers are relatively thin, they are modelled together with the sclera and the optic nerve as a single homogenous region. The thermal conductivities of the sclera, vitreous, lens, aqueous humour, iris and cornea have been already mentioned in the last section. Each of these regions is assumed to be thermally isotropic and homogeneous.

The governing equation used for heat flow in the eye is the Pennes bio-heat equation [18]:

$$\rho_t C_t \frac{\partial T_t}{\partial t} = \nabla\left(k\nabla T\right) + \omega\rho_b C_b\left(T_{a,in} - T_{v,out}\right) + Q \qquad (1)$$

Heat generation is due to metabolism or external sources such as radiation of electromagnetic waves.

Assumptions

The first two terms on the right hand side of the bio-heat equation account for heat transfer due to conduction and blood perfusion through the eye, respectively. Because only a small part of the entire eye is nourished by blood supply and has metabolic activity, the second and third terms of the equation can be neglected, yielding the final governing equation:

$$\rho_t C_t \frac{\partial T_t}{\partial t} = k\nabla^2 T \qquad (2)$$

Where ∇^2 denotes the Laplacian operator.

For a steady state solution with no external heat sources, equation (2) reduces down to:

$$k\nabla^2 T = 0 \qquad (3)$$

Moreover properties of the fluids i.e., air; blood, aqueous humour and vitreous humour (its ρ, μ, C and k) are kept constant in all the equations.

Properties and thermal behaviour of the eye have been assumed to be symmetric about the pupillary axis.

Boundary Conditions

The boundary conditions can be represented by figure 4. The cornea is the only region in the eye that is exposed to the environment. At an ambient temperature lower than the corneal surface temperature, heat is extracted away from the eye via convection and radiation. A layer of tear film sits on top of the cornea. This layer is constantly evaporated and refreshed through the blinking of the eye lids. Besides convection and radiation, the evaporation of tears increases the cooling rate on the corneal surface. The loss of heat from the cornea generates a flow of heat flux from the regions of higher temperature inside the eye to the corneal surface. Thus, the boundary condition on the corneal surface (exterior boundary of the Cornea) may be shown as [6]:

$$-k_1 \frac{\partial T_1}{\partial n} = h_{ambient}(T_1 - T_{ambient}) + \varepsilon\sigma(T_1^4 - T_{ambient}^4) + E \qquad (4)$$

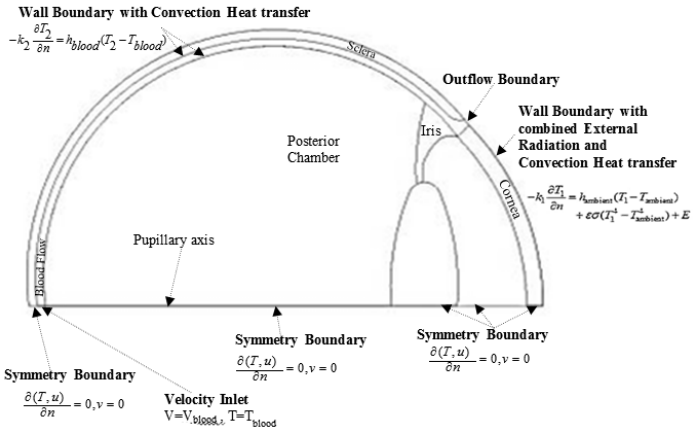

Figure 4 Representation of the 2D Model with exterior boundary conditions.

Where $\partial T_1/\partial n$ is the rate of change of temperature T_1 in the direction of the outward unit vector to corneal boundary, it is to be noted here that the non-linear term models the heat transfer process by radiation.

On the boundary that blood flow channel shares with the eye tissues (i.e., Cornea, Iris, Posterior chamber and Sclera) heat enters the eye system through the flow of blood. This may be modelled by using the boundary condition:

$$-k_2 \frac{\partial T_2}{\partial n} = h_{blood}(T_2 - T_{blood}) \qquad (5)$$

Where $\partial T_2/\partial n$ is the rate of change of temperature T_2 in the direction of the outward unit vector to boundary.

Velocity Inlet at the inlet of blood flow:

$$V = V_{blood}, T = T_{blood} \qquad (6)$$

Direction of velocity vector is normal to the velocity inlet boundary.

Symmetry Boundary Condition at the pupillary axis:

$$\frac{\partial(T,u)}{\partial n} = 0, v = 0 \qquad (7)$$

Where the partial derivative term represents rate of change of flux in the direction of outward unit vector to the pupillary axis.

The approximate values of control parameters related to boundary conditions are shown below in table 2 [6]:

Table 2 Control parameters for exterior boundary conditions

Control Parameter	Value
Blood Temperature T_{blood} (˚C)	37
Ambient Temperature $T_{ambient}$ (˚C)	25
Emissivity of Cornea ε	0.975
Blood Convection Coefficient h_{blood} ($Wm^{-2}(˚C)^{-1}$)	65
Ambient Convection Coefficient $h_{ambient}$ ($Wm^{-2}(˚C)^{-1}$)	10
Heat flux loss due to tear evaporation E(Wm^{-2})	40
Stefan-Boltzmann Constant σ ($Wm^{-2}(˚C)^{-4}$)	$5.67x10^{-8}$

Method Adopted For Meshing

With an assumption that properties and thermal behavior of eye is symmetric about the pupillary axis, a two dimensional model of the eye has been prepared in CATIA V5 R18.The model is basically a surface model with the entire geometrical model divided into 7 sections. The sections being Cornea, Anterior chamber (Aqueous Humour), Lens, Iris, Posterior Chamber (Vitreous Humour) and Sclera. Figure 5 represents the model. It has to be noted here that the structure of the iris has been simplified for the purpose of ensuring a better quality of mesh and more precise results, although the shape selection for Iris is based upon the optimization of the existing form used by different authors. Here the sclera has been split into two sections with the inner section depicting blood flow into and out of the eye. The model is then meshed in ANSYS 14.0 using ICEM CFD mesher. Each surface is meshed individually and material properties have been successfully applied to each of the sections. The mesh developed is a tetra mesh with most of the elements being Quad while some of them of Tri nature. Figure 6 represents the meshed model. Subsequently boundary conditions have been applied accordingly as already mentioned in mathematical modeling section i.e., on the outer boundary of Cornea and on the interface that the blood flow channel shares with Sclera, Posterior chamber containing Vitreous Humour ,Iris and Cornea.

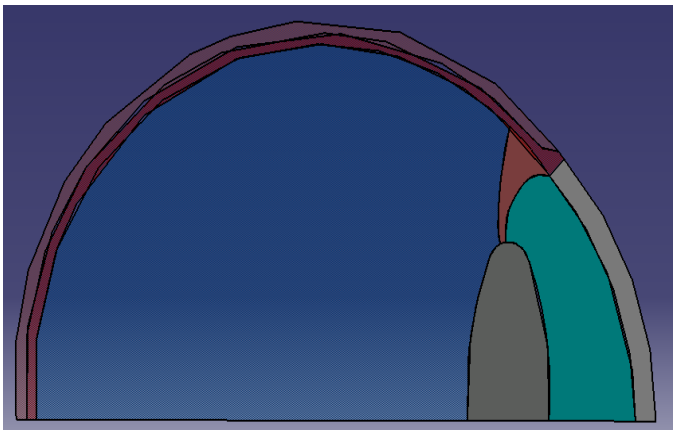

Figure 5 2D Geometric Model of the eye .

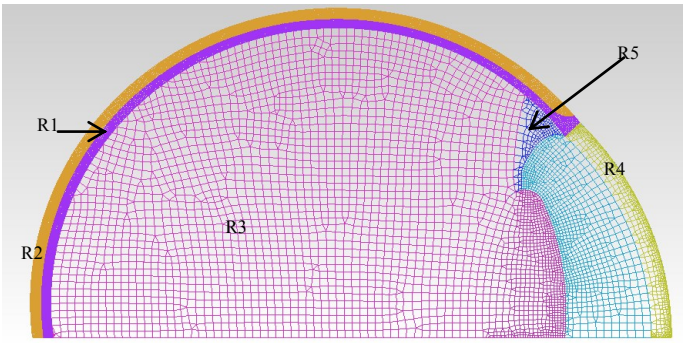

Figure 6 2D Mesh generated for the model-View in ANSYS ICEM CFD 14.0.

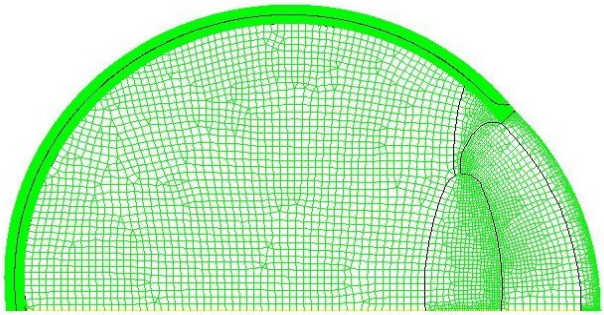

Figure 7 2D Mesh generated for the model-View in Fluent 14.0

So, on the outer boundary of region R4 in figure 6 - boundary condition WALL has been applied with mixed convection and radiation conditions which represents heat transfer from the boundary by both convection and radiation. The lowermost boundary of region R1 in figure 6 has been assigned boundary condition Velocity-Inlet with inlet blood flow velocity V_{blood} of 6.2cm/s corresponding to mean arterial pressure of 80 mm Hg as is evident from figure 8[19]. The uppermost section of region R1 which is in the form of an arc as a continuation for the outer boundary of Sclera i.e., region R2, has been assigned boundary condition OUTFLOW resembling blood outflow. The inner boundary of region R1 shared by regions R2, R3 and R5 have been assigned boundary condition WALL with convective heat transfer which likewise represents heat transfer from the boundary of region R1 to regions R2,R3 and R5 by convection . The solver model makes use of an energy equation which is equivalent to the mathematical Pennes Bioheat Equation [18] i.e., equation (1).Although the hydraulic diameter of the blood vessels is very small which unanimously with its density and viscosity may yield a low Reynolds Number which is indicative of laminar flow, however the flow becomes fully developed turbulent flow as blood enters the eye so the Viscous model used is standard k-Epsilon turbulent model which makes use of two standard equations. This model allows the determination of both turbulent length and time scale by solving two separate transport equations. Moreover the model has been quite popular in its application in practical flow calculations. The flow calculations have been performed using a Pressure based solver which enables the Pressure-based Navier Stokes solution algorithm. Since steady state temperature distribution is being

studied so conditions that correspond to a steady flow are being solved.

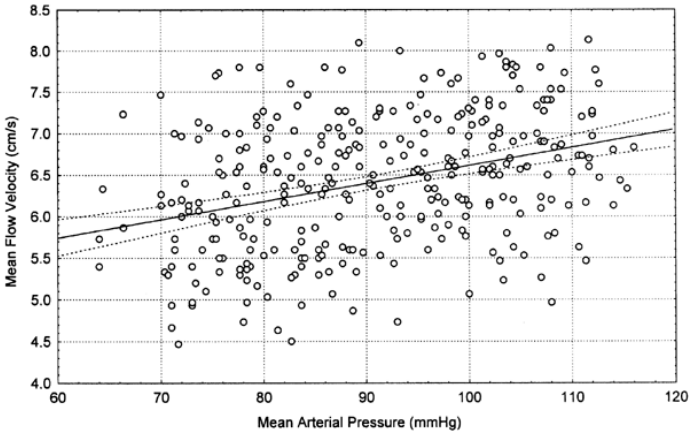

Figure 8 Variation of mean flow velocity with mean Arterial Pressure.

NUMERICAL SOLUTION PROCEDURE

With regards to the solution procedure two-dimensional equations of mass, momentum and energy have been integrated over the control volume and the subsequent equations have been discretized over the control volume using Finite Volume technique to yield a set of algebraic equations which could be solved by the algebraic multi grid solver of **Fluent 14.0** in an iterative manner by imposing the above boundary conditions. Second order upwind scheme (for convective variables) was considered for the momentum as well as for the discretized equations of energy. After a first-hand converged solution could be obtained (with 32000 cells) with 325 iterations, the grids throughout were coarsened to half of its size (total cells = 16000), the cell dimension was made half in both the directions so that the numerical errors can reduce very much, and the solution process was again made to converge at 210 iterations where it was seen that the corneal temperature at the centre changed by 0.26%. Then a second round of refinement in grids was done over the geometry which resulted in 80000 cells in total and the corneal temperature at the centre changed only by 0.16%. Then a second order upwind scheme was adopted for the final convergence of the equations where the corneal temperature at the centre hardly changed. This average value is reported and has been used for the correlation to predict the corneal temperature.

Semi-Implicit Method for the Pressure Linked Equations (SIMPLE) algorithm with a Standard scheme for the pressure interpolation (to find cell face pressure from cell center pressure) was used for the pressure correction equation. Under relaxation factors of 0.5 for pressure, 0.7 for momentum and 1 for energy were used for the convergence of all the variables. Convergence of the discretized equations were said to have been achieved when the whole field residual for all the variables fell below 10^{-3} for u, v, and p (since these are non-linear equations) whereas for energy the residual level fell to 10^{-6}.

RESULTS AND DISCUSSION

Grid Independence Test

The grid sensitivity of the solution process has been studied in the numerical procedure as discussed in the last section. In Fig.9 temperature at the centre of the cornea has been shown at three sections along the thickness, i.e., the outermost section exposed to environment, middle section and the innermost section the corneal layer have been shown as a function of grid refinement or number of cells. The conditions of simulation has been same for all the cell sizes i.e., body temperature of 310K which corresponds to the inlet fluid temperature, environmental temperature of 298K and blood flow velocity of 0.62m/s. After a cell size of 16000, the corneal temperature decreases slowly and after 32000, there is hardly any change in the corneal temperature at the centre at all the three sections when the total cells is increased from 32000 to 127000 through 80000. For our computation the results corresponding to 127000 has been adopted owing to the fact that the results are practically not changing after 32000 cells nevertheless, with refinement the results are having a tendency to become more precise thus yielding a pretty accurate corneal temperature distribution.

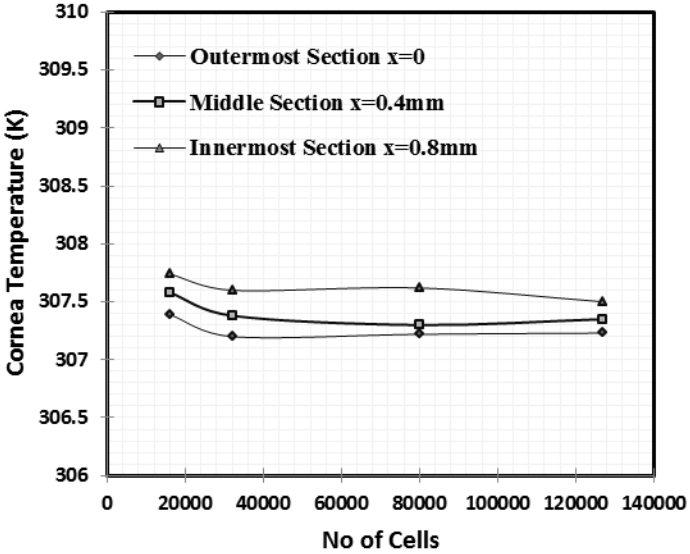

Figure 9 Corneal Temperature as a function of grid size at three sections of the corneal layer.

Temperature Distribution within Eye

Based on the grid independence test the static temperature distribution for grid sizes of 16000, 32000 and 127000 are shown in figure 10, figure 11 and figure 12 respectively. Moreover plots for temperature distribution across centerline of Cornea is shown for the three grid sizes in figure 13, figure 14 and figure 15 respectively.

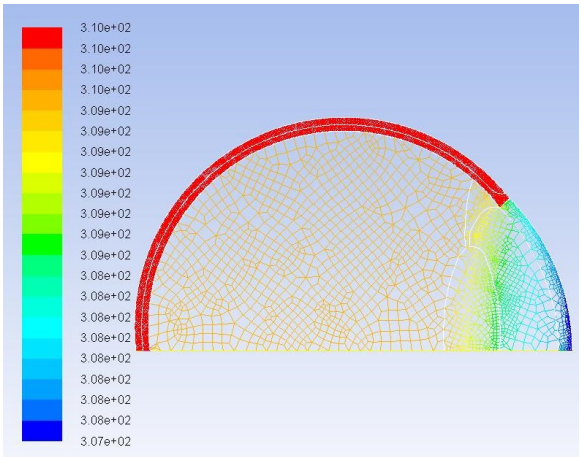

Figure 10 Contours of Static Temperature (K) corresponding to grid size of 16000.

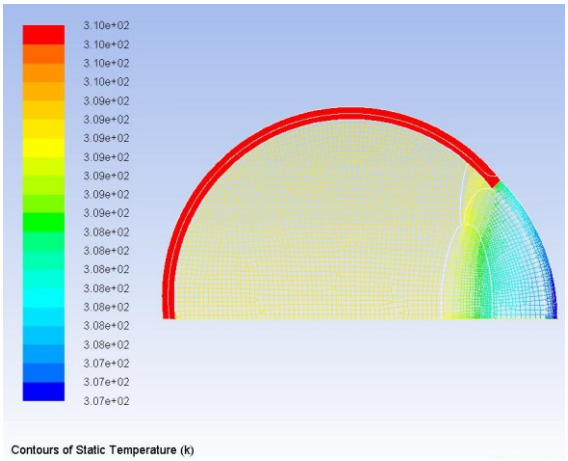

Figure 11 Contours of Static Temperature (K) corresponding to grid size of 32000.

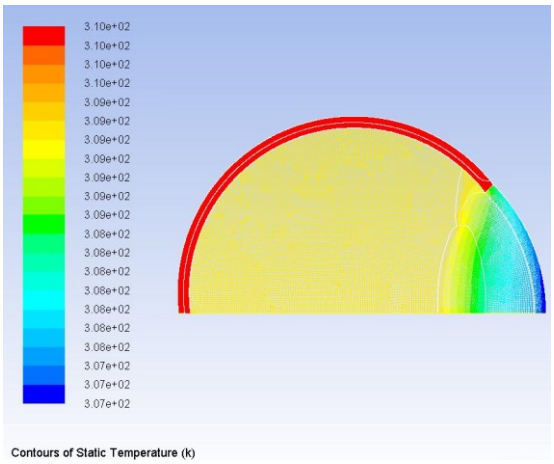

Figure 12 Contours of Static Temperature (K) corresponding to grid size of 127000.

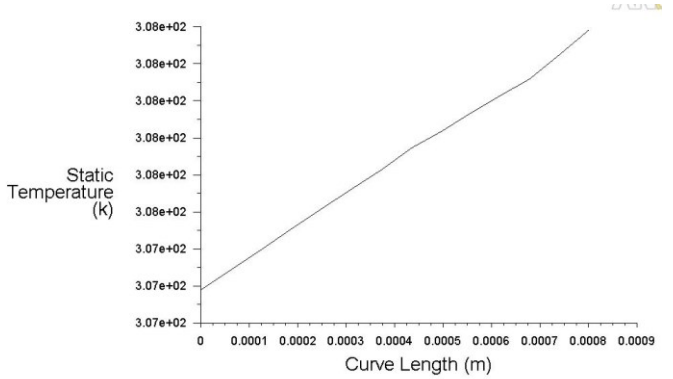

Figure 13 Plot of Static Temperature (K) v/s Curve length (m) at the centre of the cornea across the thickness corresponding to grid size of 16000(X=0 being outermost section of the cornea).

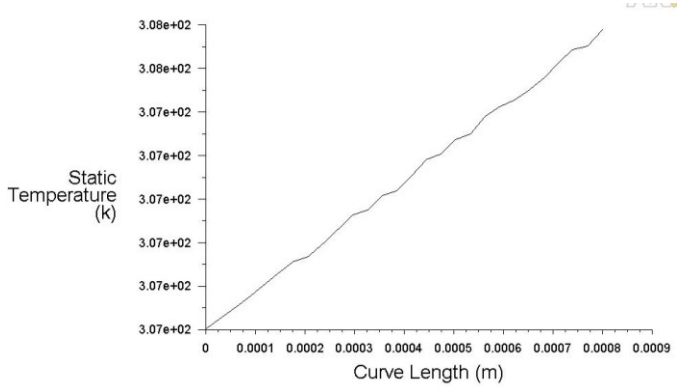

Figure 14 Plot of Static Temperature (K) v/s Curve length (m) at the centre of the cornea across the thickness corresponding to grid size of 32000(X=0 being outermost section of the cornea).

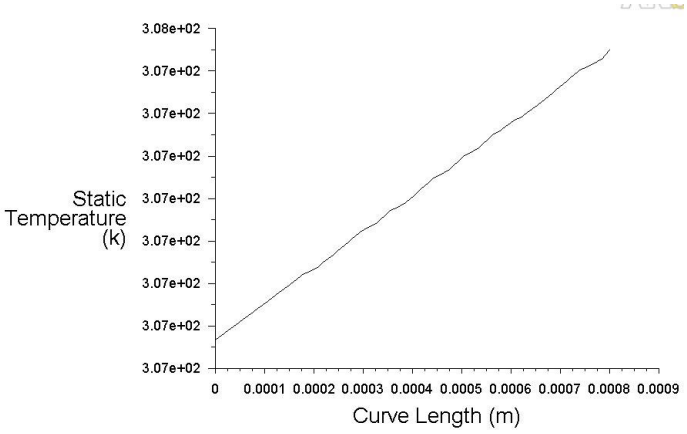

Figure 15 Plot of Static Temperature (K) v/s Curve length (m) at the centre of the cornea across the thickness corresponding to grid size of 127000(X=0 being outermost section of the cornea).

As is evident from the above figures, there is a variation of around 0.27˚C across the centerline of cornea with a temperature of 307.23K on the outer surface. Thus there is a

temperature variation from 34.23˚C to 34.5 ˚C from outer surface to inner surface of the cornea.

When a comparison is made with the results of other computation techniques it is found that there is a small difference in the corneal temperature with a discrepancy of 1.4% with the works of Ng & Ooi involving Finite element method [7] and boundary element method [6] respectively. With Amara [20] the discrepancy is 1.2%, while the discrepancy elevates to 2.8% with Scott [9]. The variation in results amounts to 0.56% with the Web Spline technique used by Kunter and Seker [10]. Now, with respect to the experimental results, our result exhibits a discrepancy of 0.86% with that of corneal temperature suggested by Mapstone [12]. The thermography method used by Rysä and Sarvaranta[21] shows a variation of 0.78% with the current result while the variation is 0.5% with the experimental results of Fielder et al.[22]. The variation in the results amounts to 0.2% with the results of Efron, Young and Brennan [23].Moreover figure 16 shows the temperature distribution along the pupillary axis with the lowest being at the corneal surface and the highest being at the Sclera.

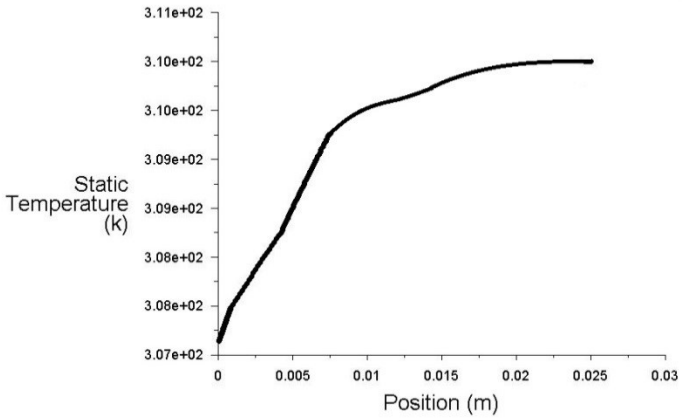

Figure 16 Plot for Static Temperature (K) v/s Position (m) along the pupillary axis.

The plot very clearly indicates that the temperature increases steeply up to the interface separating the lens from vitreous humour, however the temperature further increases at a decelerated rate up to sclera. Thus an appreciable temperature gradient exists across the pupillary axis of eye. Another aspect of our study has been to focus on the variation in the corneal temperature as the body temperature rises say, in case of fever. To study the effect of increasing temperature, simulations were run with increment in temperature from 98.6˚F i.e. the normal body temperature followed by 99 ˚F then increment in steps of 1 ˚F up to 104 ˚F which corresponds to 313K. Figure 17 depicts the variation in the outer and inner surface temperature of Cornea with increasing core body temperature. Thus we see that at a body temperature of 103 or 104 ˚F the temperature gradient across the corneal layer is around 1.2 ˚F. These values of core body temperature indicate a high fever and under these conditions the susceptibility of eye to acquire infections increases.

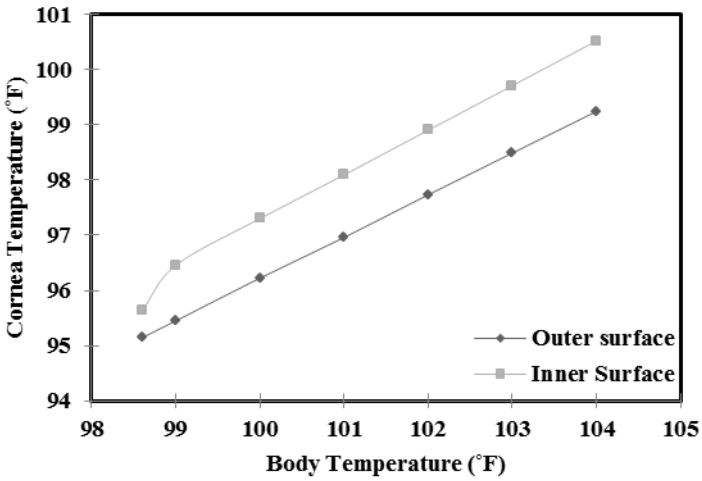

Figure 17 Plot for Body Temperature (˚F) v/s Cornea Temperature (˚F)

CONCLUSION

Thus computational fluid dynamics has been applied quite successfully on the 2D section of human eye to obtain steady state temperature distribution within the eye and especially across the corneal layer. The entire heat transfer phenomenon occurring within our eyes can be categorised into two forms i.e., absorbing heat from the blood flowing into the eye and loss of heat by convection and radiation through the corneal layer that is exposed to the environment. The approach can prove to be promising in the field of both heat transfer analysis as well as medical science. The approach can also be adopted for studying the impact of increase or decrease in the blood flow within the eye by simply changing the velocity of blood flow at the inlet while defining the boundary conditions. One drawback of the method we figured out was difficulty in representing blood flow in and out of the sclera as a result of which the scope of geometric modelling of the blood flow channel was constrained leading to a somewhat isolation of the scleral section with the rest of the eye which actually experiences both heat gain from blood and heat loss from the cornea. However, the prospects of the current study with its ability to simulate heat transfer as well as blood flow along with its close conformity with the experimental results obtained by previous studies diminishes the drawbacks whatsoever. The relationship between cornea temperature and core body temperature gives a clear indication of easy susceptibility of acquiring eye diseases at an early age if the diseased condition of the body at such high temperatures is not taken care of right away. Long intervals of such high temperature gradient across the Cornea can lead to onset of lens diseases like Presbyopia, Glaucoma etc. which are closely associated with the phenomenon of the formation of Krukenberg's Spindle as discussed earlier [2]. That is the reason that a high fever may seemingly require some eye drop to look after the cooling phenomenon of within the eye. The advantages can also be attributed to the flexibility of the software where the results with different conditions can also be studied in an effective and simple manner by merely changing the boundary condition parameters like the

surrounding temperature etc. Thus computational fluid dynamics technique appears to provide a more reliable solution for temperature distribution within the eye and is therefore an interesting and more practical alternative to other numerical techniques for heat transfer analysis in human eye.

REFERENCES

[1] Barocas VH and Heys JJ., A Boussinesq Model of Natural Convection in the Human Eye and the Formation of Krukenberg's Spindle, *Annals of Biomedical Engineering*,*Vol. 30,pp 392-401*,2002.

[2] Bergenske, P.D. Krukenberg's spindle and contact lens-induced edema. *Am. J. Optom.Physiol.* Opt. 57:932-935, 1980.

[3] Moses, R.A. "Intraocular pressure". In: *Adler's Physiology of the Eye. 6th Edition*, edited by R.A. Moses. St. Louis: C.V. Mosby Company, pp. 179-191,1975.

[4] Al-Badwaihy, K.A. and A.B.A. Youssef. "Biological thermal effect of microwave radiation on human eyes". In: Biological Effects of Electromagnetic Waves, edited by C.C. Johnson and M.L. Shore. Washington DC: DHEW Publication, pp. 61-78, 1976.

[5] Ooi EH and Ng EYK, Simulation of aqueous humour hydrodynamics in human eye heat transfer, Computers in Biology and Medicine 2008: 38.

[6] Ooi EH, Ng EYK and Ang WT, Bioheat transfer in the human eye: a boundary element approach, *Engineering Analysis with Boundary Elements*,Vol. 31,Issue 6,pp. 494-500, 2007.

[7] E.Y.K. Ng, and E.H. Ooi, "FEM Simulation of the Eye Structure with Bio-heat Analysis", *Comput. Methods Programs Biomed.* Vol. 82, No. 3, pp. 268–276, 2006.

[8] Langedijk JJW. A mathematical model to calculate temperature distributions in the human and rabbit eyes during hyper thermic treatment. *Physics in medicine and Biology,* pp.1301-1311, 1982.

[9] J.A. Scott, "A finite element model of heat transport in the human eye", *Physics in Medicine and Biology,* v33. 227-241, 1988.

[10] Kunter FC and Seker SS, Heat transfer model of human eye using web-spline technique, *Proceedings of 14th Biennial IEEE Conference on Electromagnetic Field Computation*,2010 .

[11] U. Cicekli, Computational model for heat transfer in the human eye using the finite element method, *M.Sc. Thesis, Department of Civil and Environmental Engineering, Louisiana State University*, 2003.

[12] Mapstone R, Measurement of corneal temperature. *Experimental Eye research*; Vol.7; 237-243,1968.

[13] Kampmeier J, Radt B, Birngruber R and Brinkmann R, "Thermal and Biomechanical Parameters of Porcine Cornea'',*Cornea* Vol .19(3): pp. 355-363,2000.

[14] Tanelian, D.L. and Beuerman, "Responses of Rabbit Corneal Nociceptors to Mechanical and Thermal stimulation'', *Exp Neurol.,*Vol.84, pp.165-178,1984.

[15] Chan E, Modelling heat transfer through human eye, lecture notes MAE 221A,University of California-San Diego,2007.

[16] Kiel JW and San R,"The Ocular Circulation", *Morgan and Claypool Life Sciences*, 2010.

[17] Wessapan T and Rattanadecho P, Specific Absorption Rate and Temperature Increase in Human Eye Subjected to Electromagnetic Fields at 900 MHz, *Journal of Heat Transfer, Vol. 134, Issue 9*, 2012.

[18] Pennes HH, Analysis of tissue and arterial blood temperatures in the resting forearm, Journal of Appl. Physiology, 1948.

[19] Polak K, Polska E, Luksch A, Dorner G, Fuchsjäger-Mayrl G, Findi O, Eichler HG, Wolzt M and Schmetterer L,"Choroidal Blood Flow and Arterial Blood Pressure" , Department of Ophthalmology, Austria,2003.

[20] Amara EH. Numerical investigations on thermal effects of laser ocular media interaction. *International journal of heat and mass transfer ,Vol.* 38;pp. 2479-2488,1995.

[21] Rysä P and Sarvaranta J, Thermography of eye during cold stress, *Acta Ophthalmologica*,Vol.123, pp. 234-239, 1973.

[22] Fielder AR, Winder AF, Sheraidah GA and Cooke ED, Problems with Corneal Arcus, *Transactions of the ophthalmological societies of United Kingdom,Vol.101(1),pp.* 22-26, 1981.

[23] Efron N, Young G and Brennan N, Ocular Surface Temperature, *Current Eye Research*, Vol. 8(9),pp. 901-906, 1989.